Report of Investigations 7867

Toxic Fumes From Explosives: Ammonium Nitrate-Fuel Oil Mixtures

By R. F. Chaiken, E. B. Cook, and T. C. Ruhe
Pittsburgh Mining and Safety Research Center, Pittsburgh, Pa.

Note: This is a reference cited in *AP 42, Compilation of Air Pollutant Emission Factors, Volume I Stationary Point and Area Sources.* AP42 is located on the EPA web site at www.epa.gov/ttn/chief/ap42/

The file name refers to the reference number, the AP42 chapter and section. The file name "ref02_c01s02.pdf" would mean the reference is from AP42 chapter 1 section 2. The reference may be from a previous version of the section and no longer cited. The primary source should always be checked.

UNITED STATES DEPARTMENT OF THE INTERIOR
Rogers C. B. Morton, Secretary

BUREAU OF MINES
Thomas V. Falkie, Director

This publication has been cataloged as follows:

Chaiken, R F

Toxic fumes from explosives: ammonium nitrate-fuel oil mixtures, by R. F. Chaiken, E. B. Cook, and T. C. Ruhe. [Washington] U.S. Bureau of Mines [1974]

24 p. illus., tables. (U.S. Bureau of Mines. Report of investigations 7867)

Includes bibliography.

1. Explosives. 2. Fume control. I. U.S. Bureau of Mines. II. Cook, Edwin B., jt. auth. III. Ruhe, T. C., jt. auth. IV. Title. V. Title: Ammonium nitrate-fuel oil mixtures. (Series)

TN23.U7 no. 7867 622.06173

U.S. Dept. of the Int. Library

CONTENTS

	Page
Abstract	1
Introduction	1
Acknowledgments	3
Theoretical considerations	3
Kinetics of NO and CO in expansion	3
Calculation of the detonation state of AN-FO	4
Experimental determination of toxic fumes	8
Large closed-gallery system	8
Gas analysis	10
Explosive charge design	10
Measurement of detonation velocity	11
Results and discussion	16
Conclusions and recommendations	22
References	23

ILLUSTRATIONS

1.	Bureau of Mines large closed-gallery facility	8
2.	Experimental devices	9
3.	Decay of detonation velocity AN-FO (prilled) (94 to 6)	13
4.	Decay of detonation velocity AN-FO (pulverized) (94 to 6)	13
5.	Decay of detonation velocity catalyzed AN-FO (96 to 4) (equivalent)	14
6.	Decay of shock velocity sand (inert charge)	14
7.	Toxic fumes from AN-FO mixtures, gallery and theoretical results	15
8.	Toxic fumes from AN-FO mixtures, gallery and Crawshaw-Jones results	15
9.	Toxic fumes from AN-FO mixtures, carbon monoxide	16
10.	Variation of velocity decay constant with variation in percent fuel oil	21
11.	Variation of detonation velocity at 14 cm with variation in percent of fuel oil	21

TABLES

1.	Comparison of calculated ideal detonation properties for AN-FO (94 to 6)	5
2.	Ideal detonation properties of AN-FO $NH_4NO_3/C_{7.17}H_{14}$; ρ_o = 0.8 g/cm^3	7
3.	Large closed-gallery results for prill and pulverized AN-FO mixtures	17
4.	Crawshaw-Jones test results for pulverized AN-FO mixtures	18
5.	Comparison of predicted and experimental NO/NO_2 ratios for pulverized AN-FO	19

TOXIC FUMES FROM EXPLOSIVES: AMMONIUM NITRATE-FUEL OIL MIXTURES

by

R. F. Chaiken,[1] E. B. Cook,[2] and T. C. Ruhe[3]

ABSTRACT

The Bureau of Mines has carried out experimental and theoretical studies with prilled and pulverized ammonium nitrate-fuel oil (AN-FO) mixtures containing varying amounts of fuel oil in an attempt to quantify the effects of stoichiometric composition, nonideal detonation behavior, and expansion volume on the production of CO, NO, and NO_2 fumes. Experimental fume measurements were obtained in the Bureau's large closed gallery facility (7.2×10^4 liter expansion chamber) and in the standard Crawshaw-Jones apparatus (90-liter expansion chamber) using a prepackaged charge configuration containing about 450 g of explosive.[4] The theoretical calculation of toxic fumes was achieved with an equilibrium detonation code called "TIGER."

Contrary to initial expectations, the NO_x (= NO + NO_2) fumes from the large gallery test were found to be in essential agreement with the Crawshaw-Jones results. It was also concluded that (1) "TIGER" calculations offer a good approach to the prediction of toxic fumes; (2) there is a basic problem in extrapolating laboratory measurements of CO fumes to mine conditions--this being due to postdetonation oxidation of CO to CO_2; and (3) the detonation velocity decay rate of an explosive is a useful experimental parameter for correlating toxic fumes production with nonideal detonation behavior.

INTRODUCTION

The potential hazards of fumes from blasting operations in underground mines have long been recognized. These hazards stem from the fact that when agents such as dynamite and ammonium nitrate-fuel oil mixtures (AN-FO) detonate, small (1 to 5 wt-pct) but significant amounts of CO, NO, and NO_2 are liberated as detonation products. Under limited ventilation conditions, such as those which could exist in a mine, these detonation products can present a severe toxic fume hazard to mine workers. This is particularly true with NO_2

[1] Research chemist.
[2] Research chemist (now retired).
[3] Chemist.
[4] The term explosive in this paper will refer to both "explosives" and blasting agents.

which has a lethal toxicity (~220 ppm) and threshold limit value (5 ppm) comparable to that of hydrogen cyanide (15).[5]

There have been numerous measurements made of NO_x (that is, NO + NO_2) and CO in underground mines from ammonium nitrate-based explosives and indeed hazardous concentration levels have been found (12, 14, 18, 22-23). The quality and quantity of fumes produced appears to depend upon a number of factors such as explosive composition, product expansion, method of priming, length of charge, and confinement. Unfortunately, the difficulties in controlling the experimental conditions in a mine make it difficult to quantitatively assess the relationship between toxic fumes and the factors that influence their production.

Laboratory determinations of toxic fumes from explosives have also been carried out (7, 12, 14, 16, 18, 19, 22-23). The experiments generally consist of detonating a small quantity (100 to 500 g) of explosive in a closed chamber, followed by sampling and analysis of the residual fumes. The Crawshaw-Jones test (90-1 chamber) (10, 19), the Bichel Gage test (14.5-1 chamber) (10, 18), and the Dolgov Bomb test (50-1 chamber) (1) are typical of the types of apparatus used. Explosive confinements have included bare charges, cement blocks, and steel cannon boreholes with and without stemming. For AN-FO and other explosives, the values of NO_x produced in the laboratory have been found to be less than those obtained in the mine (16, 18, 22-23).

There are several problems inherent to the laboratory experiments which likewise make it difficult to obtain toxic fume data that can be related to explosive composition and extrapolated to mine conditions. First, it is difficult to achieve consistent detonation in relatively small quantities of blasting agents such as AN-FO. The degree of confinement plays an important role in determining the detonation state condition and work performed, and hence could affect the composition of the expanded products.

Second, product expansion of detonation products to near 1 atm residual pressure requires a sizable expansion chamber even for small quantities of explosive (about 10^3 to 1 for an evacuated chamber and about 10^4 to 1 for an atmospheric chamber). The resulting large volume dilution of fumes imposes severe sensitivity requirements on the gas sampling and analytical techniques. Product expansions leading to higher residual pressure (that is, small expansion volumes) could lead to condensation of water from the detonation products, and removal of NO_x fumes by absorption. The higher surface-to-volume ratio of small expansion chambers would enhance this effect.

The Bureau of Mines has been investigating toxic fume production with AN-FO mixtures from the viewpoint of resolving the above laboratory test problems, while attempting to approach conditions amenable for theoretical analysis of the effect of mixture composition on NO_x and CO fume production. The current work, which extends previous studies in the Crawshaw-Jones apparatus (19, 23), was made possible by the following recent developments:

[5]Underlined numbers in parentheses refer to items in the list of references at the end of this report.

(1) Availability of a large, closed explosion gallery facility (7.2×10^4 l expansion chamber), (2) a new chemiluminescent technique for measuring small quantities (as low as 0.1 ppm) of NO and NO_2, (3) a new equilibrium computer code for calculating products of detonation, and (4) recent theoretical treatments of the kinetics of NO and CO reaction in combustion systems.

It is the purpose of this report to describe these developments and the test results obtained with AN-FO mixtures containing varying amounts of fuel oil.

ACKNOWLEDGMENTS

A number of people at the Bureau contributed directly to the work of this report and their efforts are gratefully acknowledged. Helen Lang and her colleagues in the Bureau's Analytical Research Group carried out many gas chromatographic and wet colorimetric analyses. John Nickovich and Paul Richardson did much of the work of converting the large gallery to a toxic fume test facility. Robert McNall and Ronald Brewer gave able assistance in the design and firing of the explosive charges. Elva Guastini helped prepare the explosive charges. And Dr. Charles M. Mason, research chemist, engaged in helpful discussion of the results of the work.

THEORETICAL CONSIDERATIONS

Kinetics of NO and CO in Expansion

The detonation of a stoichiometric AN-FO mixture (AN-FO mass ratio = 94.5 to 5.5) can be represented in gross terms by the following overall reaction:[6]

$$NH_4NO_3 + 0.0469\ C_{7.17}H_{14} \rightarrow N_2 + 2.328\ H_2O + 0.336\ CO_2.$$

Obviously the amount and type of products will change with mixtures containing nonstoichiometric amounts of fuel oil. For example, a negative oxygen balance (that is, more fuel oil) will tend to give CO rather than CO_2, while a positive oxygen balance will give some NO. However consideration of the equilibrium reactions which occur at the elevated pressure and temperature of detonation dictates that some NO, NO_2, and CO will be formed at all mixture ratios, including the 94.5 to 5.5 mixture. Some of the pertinent elementary reactions known to occur during the air combustion of hydrocarbons are the following:

$$HOH = H + OH,$$

$$N_2 = N + N,$$

$$N + OH = NO + H,$$

$$CO + OH = CO_2 + H,$$

and

$$NO + O = NO_2.$$

[6] $C_{7.17}H_{14}$ is taken as an average molecular composition for No. 2 diesel fuel.

Newhall (11) examined the kinetics of some 17 elementary reaction processes of the above type in an attempt to ascertain how rapid changes in pressure and temperature would effect the composition of exhaust gases in an internal combustion engine. Starting with an equilibrium mixture of combustion products at 2665 K and 27.2 atm, his calculations (using known kinetic constants and an ideal gas equation of state) showed that during piston expansion (~5-msec time duration) NO would be frozen at its initial concentration, and CO frozen at ~50 pct of its initial concentration. That is to say, the normal rates of equilibrium reactions leading to the reduction of NO to N_2 and the oxidation of CO to CO_2 cannot keep pace with the cooling effects of the gas expansion.

These results suggest the possibility that the NO_x and CO formed during the detonation of an explosive would remain relatively unchanged during expansion to atmospheric pressure. In the case of borehole charges of AN-FO, the temperature of the detonation products is expected to be about the same value as that considered by Newhall, the detonation pressure considerably higher ($\sim 5 \times 10^4$ atm), and the expansion time somewhat shorter (~1 msec).

With the assumption that the concentrations of NO_x and CO are frozen during expansion, the problem of theoretical prediction of toxic fume production becomes one of calculating the initial composition of the detonation products. This problem is considerably more complex than that of the internal-combustion-engine problem in that the gaseous products can no longer be adequately described by an ideal gas equation of state (EOS).

Calculation of the Detonation State of AN-FO

Utilizing the Chapman-Jouquet theory of detonation, it is possible to calculate the ideal detonation properties of an explosive provided one knows the EOS for the detonation products (17). Several computational methods have been developed during the past 25 years to achieve this goal. However, there is still considerable controversy as to the proper EOS for gas mixtures at the high pressures and temperatures (on the order of 10^5 atm and 10^3 K, respectively) encountered with condensed explosives (2, 9, 17, 24).

In the current studies, a hydrodynamic-thermodynamic equilibrium code called "TIGER" (24) was employed along with various gaseous equations of state to obtain what are believed to be reasonable predictions for the ideal detonation state of AN-FO. "TIGER" is designed to solve simultaneously the hydrodynamic equations of one dimensional steady-state detonation (that is, Chapman-Jouquet theory) and the thermodynamic equations of chemical equilibrium for gas-solid mixtures. One of the distinct advantages of "TIGER" over previous

codes of its type is that different EOS subroutines can be readily programed for use.[7]

Table 1 compares the ideal detonation properties for ammonium nitrate-octane (94 to 6) using different gaseous equations of state having the form

$$\frac{PV}{\Sigma n_i RT} = \Phi(T,V,n_i), \tag{1}$$

where P is pressure, V is volume, R is the gas constant, T is temperature, n_i is the number of moles of the ith product, and Φ is a compressibility factor (equal to unity for an ideal gas).

TABLE 1. - Comparison of calculated ideal detonation properties for AN-FO (94 to 6)

	Equation of state (EOS)[1]			Experimental
	BKW/LRL[2]	BKW/Bureau of Mines[3]	Virial	
ρ_o.....g/cm..	1.0	1.0	1.0	[4]0.88
D.....m/sec..	6320	4870	4100	[4]~4700
P.....atm, 10^3..	106	67.6	48.2	[4]50-70
T.....K..	1930	2360	3230	-
Q.....cal/g..	916	904	908	-
H_2O.....moles/kg..	27.42	27.69	27.47	-
N_2.....	11.56	11.70	11.54	-
CO_2.....	3.71	3.34	3.53	-
CO.....	0.389	0.866	0.673	[5]0.8
NO.....	5×10^{-6}	3×10^{-4}	0.02	[5]0.07
NO_2.....	0	4×10^{-8}	-	-
NH_3.....	0.360	0.092	0.392	-
Total gas.....	43.59	44.06	43.78	-

[1] In these calculations n-octane was used instead of No. 2 diesel fuel.
[2] EOS parameters: $\alpha = 0.5$, $\beta = 0.1$, $\kappa = 11.85$, $\theta = 400$.
[3] EOS parameters: $\alpha = 0.5$, $\beta = 0.2$, $\kappa = 5.9$, $\theta = 400$.
[4] References 20 and 21.
[5] Estimated from current work.

For the Becker-Kistiakowsky-Wilson (BKW) equation of state (3)

$$\Phi = 1 + xe^{\beta x}, \tag{2}$$

and

$$x = \frac{\kappa \Sigma n_i k_i}{V(T+\theta)^{\alpha}} \tag{3}$$

[7] The "TIGER C" code in use by the Bureau of Mines was obtained from the U.S. Army Ballistic Research Laboratory, Aberdeen, Md. The code deck as received included the EOS subroutines used in the current study, and a "STARFIT" code which is used to generate a thermodynamic data file. Changes have been made in the data file so that the thermodynamic input data is more consistent (but not identical) with the NASA/Lewis detonation code (6). The current file at the Bureau is referred to as the "Cook File" and like its predecessors has its basic origin in the JANAF Thermodynamic Tables (4).

where the k_i's are covolumes, and α, β, κ, θ are constant parameters. The parameters for the BKW/LRL[8] EOS (table 1) have been fitted to experimental velocity and pressure data on high explosives such as RDX (cyclotrimethylene trinitramine). This EOS has in the past been used extensively for calculating detonation velocity and pressure. The parameters for the BKW/Bureau of Mines EOS have been chosen to yield detonation velocities and pressures more consistent with experimental data on AN-FO (20-21).

For the virial EOS (8);

$$\Phi = 1 + \frac{B(T,n_i)}{V} + \frac{C(T,n_i)}{V^2}, \tag{4}$$

$$B(T,n_i) = \sum_{ij} B_{ij}(T) n_i n_j, \tag{5}$$

and

$$C(T,n_i) = \sum_{ijk} C_{ijk}(T) n_i n_j n_k. \tag{6}$$

In "TIGER," the second and third virial coefficients, B(T) and C(T), respectively, correspond to a Leonard-Jones (6-12) intermolecular potential. The mixture rules for defining B_{ij} and C_{ijk} are those suggested by Hirschfelder and coworkers (8). This EOS has only recently been programed for use with TIGER. (See footnote on page 5.)

Examination of table 1 reveals that the BKW EOS is inadequate for calculating toxic fume production. Our calculations with the LRL and the Bureau of Mines parameters, as well as other values of α, β, κ, and θ indicate that the predicted NO_x fumes fall well below the experimental values. This occurs even with other AN-FO compositions and other explosives (for example, pentaerythritol tetranitrate, PETN). It was, therefore, concluded that the BKW EOS is not applicable to the problem under current consideration. Indeed, the fact that a drastic change in the LRL parameters was required in order to match the experimental detonation velocity and pressure for AN-FO suggests that the BKW EOS is merely an empirical relation having a limited application.

The virial EOS appears to yield reasonable values for velocity, pressure, and product composition, although the values for D, detonation velocity, and P, pressure, are about 15 pct too low. This latter discrepancy is even more apparent in calculations involving higher density explosives. However, of the two types of EOS currently available and tested, it is believed that the virial EOS represents a more reasonable approach to predicting the effect of AN-FO composition on NO_x and CO fume production.[9]

It is noteworthy that, because the calculated NO_x concentration in combination with detonation velocity and pressure appears to be sensitive to the EOS, realistic toxic fume measurements can serve as additional test data for evaluating various proposed high-density gaseous EOS's.

Table 2 depicts the theoretical (ideal) detonation properties of 10 AN-FO compositions (0 to 10 pct fuel oil) at a bulk loading density of 0.8 gm/cm^3 as determined with "TIGER," the virial EOS, and the "Cook File." It is seen that the quantity of NO_x fume production is expected to be at a maximum between 3 and 4 pct FO, whereas the peak in detonation velocity and heat of detonation occurs at ~6 pct FO, which is on the fuel-rich side of the stoichiometric composition (94.5 to 5.5). Below 6 pct FO little CO is to be expected; but at compositions of 6 pct and higher, the CO rapidly increases.

[8]LRL refers to the Lawrence Radiation Laboratory of the University of California. (See reference 9.)

[9]Work is in progress at the Bureau to develop an improved EOS which will overcome the apparent inadequacies of the virial EOS.

TABLE 2. - Ideal detonation properties[1] of AN-FO

$NH_4NO_3/C_{7.17}H_{14}$; ρ_o = 0.8 g/cm³

(ΔH°_{AN} = -88 Kcal/mole;
ΔH°_{FO} = -45 Kcal/mole)

Percent FO	0	1	2	3	4	5	6	7	8	9	10
D.....m/sec..	3030	3230	3410	3570	3720	3870	3980	3980	3970	3940	3910
P.....atm 10^3..	20.2	23.4	26.3	29.1	31.8	34.4	36.1	36.3	36.2	36.0	35.7
T.....K..	1890	2150	2390	2620	2850	3080	3170	3080	2990	2900	2820
V.....cm^3/g..	0.902	0.896	0.891	0.888	0.887	0.887	0.888	0.888	0.886	0.883	0.881
Q_{det}[2]...cal/g..	365	459	554	650	749	851	898	862	728	799	772
DETONATION PRODUCT COMPOSITION, MOLES/kg[3]											
H_2O.....	25.0	25.4	25.9	26.3	26.8	27.2	27.4	26.9	26.2	25.5	24.7
N_2.....	12.3	12.1	11.9	11.7	11.6	11.6	11.7	11.4	11.1	10.7	10.3
O_2.....	6.06	4.82	3.59	2.40	1.29	0.340	0.002	10^{-4}	2×10^{-5}	6×10^{-6}	2×10^{-6}
H_2.....	7×10^{-6}	5×10^{-5}	3×10^{-4}	0.001	0.004	0.016	0.253	0.769	1.23	1.59	1.84
NO.....	0.279	0.492	0.701	0.848	0.855	0.578	0.053	0.011	0.004	0.002	0.001
NO_2.....	0.047	0.049	0.046	0.036	0.022	0.007	5×10^{-6}	2×10^{-6}	4×10^{-7}	10^{-7}	4×10^{-8}
N_2O.....	0.001	0.002	0.003	0.004	0.004	0.003	3×10^{-4}	5×10^{-5}	2×10^{-5}	9×10^{-6}	5×10^{-6}
NH_3.....	2×10^{-8}	4×10^{-7}	3×10^{-6}	2×10^{-5}	10^{-4}	8×10^{-4}	0.050	0.299	0.687	1.12	1.53
O.....	2×10^{-5}	10^{-4}	4×10^{-4}	9×10^{-4}	0.002	0.002	2×10^{-4}	3×10^{-5}	10^{-5}	4×10^{-6}	0
OH.....	7×10^{-4}	0.002	0.005	0.009	0.015	0.017	0.006	0.002	0.001	6×10^{-4}	4×10^{-4}
H.....	0	0	0	0	0	0	0	0	0	0	0
CO_2.....	-	0.715	1.43	2.14	2.85	3.53	3.53	2.97	2.65	2.48	2.39
CO.....	-	2×10^{-5}	3×10^{-4}	0.002	0.008	0.046	0.761	2.00	2.96	3.68	4.23
HCN.....	-	0	-	-	-	2×10^{-6}	0.002	0.027	0.093	0.187	0.290
CH_4.....	-	0	-	-	-	0	2×10^{-5}	0.003	0.024	0.094	0.239
C.....	-	-	-	-	-	0	0	0	0	0	0
Total gas.....	43.7	43.6	43.5	43.4	43.4	43.3	43.7	44.4	45.0	45.3	45.6
C (solid).....	-	-	-	-	-	0	0	0	0	0	0

[1] "TIGER" calculations with virial equation of state.

[2] Heat of detonation.

[3] (ft^3/lb) = (moles/kg) multiplied by 0.36.

EXPERIMENTAL DETERMINATION OF TOXIC FUMES

Large Closed-Gallery System

The procedures for determining toxic fume production from explosives are in principal quite simple, namely detonating a given weight of explosive, expanding the gases produced into a known closed volume, and then sampling and analyzing the gas. However, the problem is to obtain data which can be meaningfully interpreted in terms of pertinent explosive parameters and extrapolated to mine conditions. The problem requires stringent control of the explosive geometry, the conditions of detonation, and the loss of fumes by wall effects (adsorption).

In the current work, the Bureau's large closed-gallery system (10) was employed. (See fig. 1.) The system consists of a cylindrical steel chamber 6-1/3 ft in diameter and 80 ft in length, having a total volume of 2,550 ft^3 (7.22×10^4 l). At one end of the chamber (that is, the end which is in the building on the right in fig. 1) is a 5-1/16-inch gasketed aperture against which the muzzle of a steel cannon (or mortar) is forced under hydraulic loading and mechanical propping. The cannon is a steel cylinder 2 ft in diameter and 3 ft in length containing a 2-1/4- by 23-in borehole set in a special

FIGURE 1. - Bureau of Mines large closed-gallery facility.

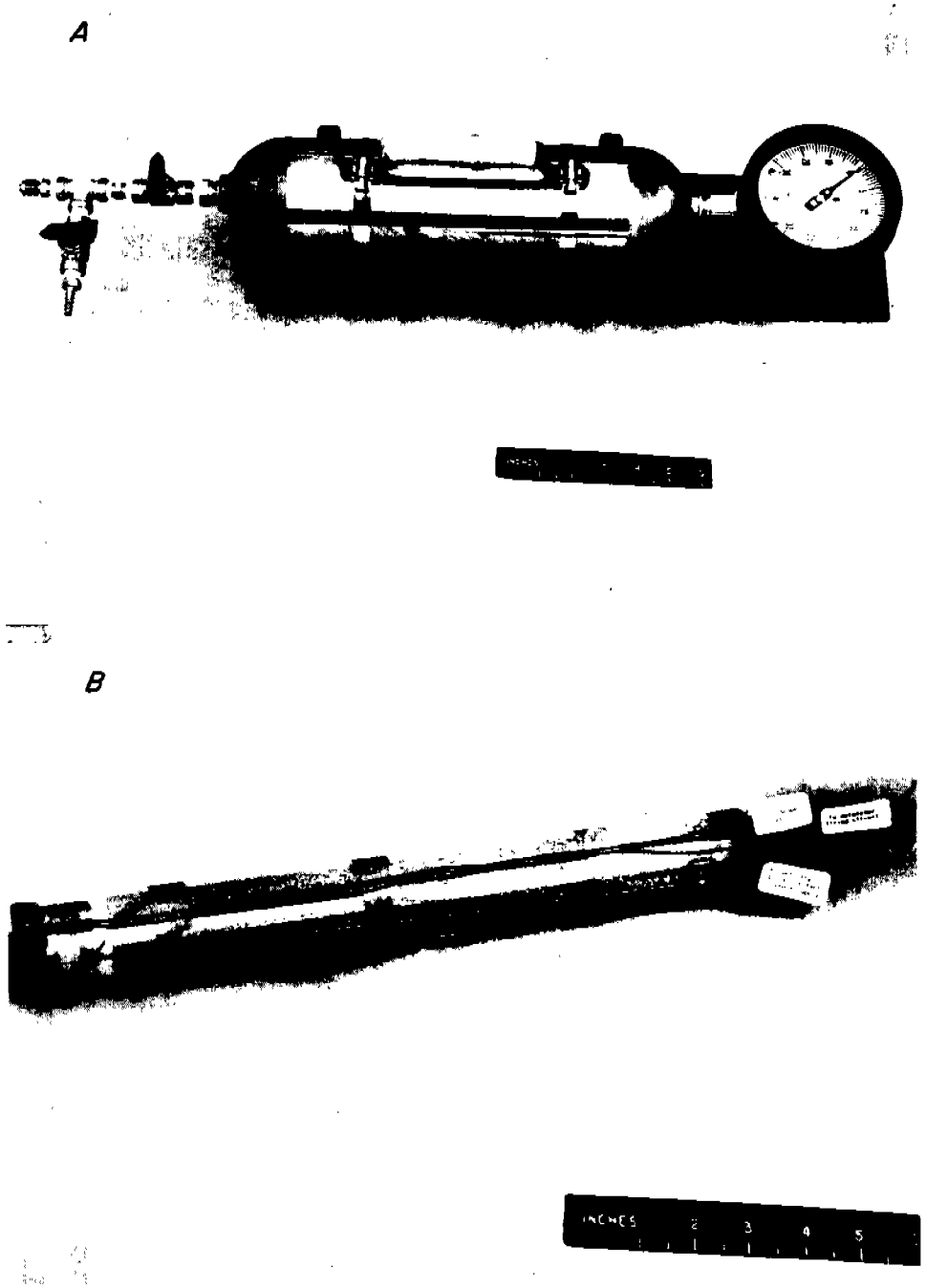

FIGURE 2. - Experimental devices. *A*, Stainless steel sampling bottle; *B*, prepackaged AN-FO charge.

steel liner. An access door at the far end of the chamber allows entry into the chamber and muzzle loading of the cannon.

The inside of the chamber is fitted with a 1,500-cfm ducted fan for stirring the gases, and an exhaust blower for airing the chamber. Three gas sampling stations are positioned at approximately 17, 44, and 68 ft along the chamber length. These consist of 3/8-in stainless steel tubes inserted through the chamber walls from an external manifold leading back to the control room. At a preset time, the gas is pumped from the chamber into a preevacuated 2.2-l stainless steel sampling bottle (fig. 2A). A combination vacuum-pressure gage on the bottle enables the gas pressure to be monitored during filling (generally at 2 atm maximum). The 304-stainless steel bottles, prior to their initial use in this work, were passivated with HNO_3 and NO_2 until no evidence of wall reaction with calibration gases could be detected (<1 pct with 15-min storage).

Tests in the large closed-gallery system showed that with 8 to 10 min stirring after shot firing, the detonation product gases were uniformly dispersed throughout the chamber.

Gas Analysis

All gas analyses were run from the 2.2-l stainless steel sample bottle filled to a pressure of ~2 atm. For CO_2, CO, CH_4, H_2, and air, standard gas chromatography was employed. Separate glass gas sample bottles of 250 cm^3 were filled from the 2.2-l steel bottle for the gas chromatographic analysis.

For the determination of NO and NO_2, a Thermoelectron Corp. model 10A chemiluminescent analyzer was employed.[10] This instrument reacts a metered flow of sample gas (taken directly from the 2.2-l stainless steel bottle) with an excess of ozone. The reaction

$$NO + O_3 \rightarrow NO_2^* + O_2$$

$$NO_2^* \rightarrow NO_2 + h\nu$$

proceeds with unit quantum efficiency, and is followed by measuring the intensity of the emitted light (5). The optical detection system is designed so that the instrument is specific to the NO_2^* chemiluminescence with a sensitivity of ~0.1 ppm, at least in the concentration range of mixtures encountered in the current studies.

To determine NO_2, the sample gas is passed through a thermal convertor unit at 650° C, that is

$$NO_2 \xrightarrow{\Delta} NO + \frac{1}{2} O_2 ,$$

prior to carrying out the ozone reaction. The NO_2 concentration is then the difference between instrument readings with and without the thermal convertor unit. Although the instrument is specific to NO, interferences can enter into the NO_2 measurement. The interference occurs because nitrogenous gases such as HNO_3 and NH_3 can also react to some extent in the thermal convertor unit to form NO. For AN-FO this problem apparently was not serious since the NO_2 determinations generally agreed with results obtained by a gas analyzer that is specific to NO_2 (Environmentrics Corp. Faristor Type N46).

Explosive Charge Design

For loading explosive into the cannon, a prepackaged, instrumented charge was used (fig. 2B). This charge design was chosen over the conventional method of bulk loading and tamping (19) in order to accomplish the following goals: (1) To maintain uniform and reproducible charge density and size, (2) to utilize a continuous velocity probe for monitoring the detonation

[10] Reference to specific trade names is made to facilitate understanding and does not imply endorsement by the Bureau of Mines.

velocity of each charge, and (3) to facilitate loading the cannon and connection of electrical leads.

The prepackaged charge is cased in a glass tube 1-3/4 in ID, 1/16 in wall thickness, and about 16 in long, cut from standard-wall 48-mm Pyrex tubing. Glass was chosen for the casing material because it is inert, rugged, and readily available. During firing the glass completely disintegrates to a fine powder which is blown from the borehole.

To assemble the charge, a booster assembly is first constructed by gluing two PETN pellets (1-5/8-in diam, 5/8-in length, having a density of 1.4 g/cm^3 and a nominal weight of 60 g) to a plaster of paris disk, 1/2 in thick having a diameter slightly smaller than the tube inner diameter. The plaster disk has a center hole to accept a No. 8 electric blasting cap. The booster assembly is then bonded (silicone rubber adhesive) into one end of the glass tube, which has been previously fitted with a Bureau type II resistance wire velocity probe (10, 13) along the length of the inside wall. The candidate explosive (nominally 430 g) is carefully poured into the tube, and sealed with a solid plaster disk at the end of the tube.

Preparation of the AN-FO mixtures involved uniform blending (in a tumbler) of No. 2 diesel fuel oil (colored red with dye) with either AN prills (American Cyanamid Corp. C-2) or pulverized AN (that is, prills which had been previously passed through a hammer mill, with average particle size of ~100 μm).

Loading the charge was accomplished from inside the gallery chamber by simply inserting the charge, detonator end first, into the cannon borehole. A free space (that is, distance between muzzle opening and end of charge) of 2 in was maintained in each case.

Measurement of Detonation Velocity

The Bureau's type II resistance wire probe is used for continuously monitoring the detonation velocity of cylindrical explosive charges. Details of the probe construction and operation can be found in references 10 and 13. Briefly, the pressure associated with the advancing detonation front collapses a thin-walled aluminum tube onto a resistance wire. The collapsing aluminum shunts an electrical current flowing through the wire causing a continuous change in voltage across the wire. The resulting voltage-time profile, which is directly related to distance-time, is recorded on an oscilloscope.

With the present explosive charge design, the detonation wave in the AN-FO is, in each case, initially overdriven by the 60-g PETN booster. Hence, the detonation velocity must decay as the detonation front passes up the charge, resulting in an oscilloscope trace which is curved rather than linear. In most instances the diameter and length of the prepackaged AN-FO charge and the degree of confinement are inadequate to establish a well-defined steady-state detonation. However, the rate of decay of the wave is a measure of the rate of rarefaction loss from the detonation reaction zone, and hence is a measure of the approach to steady-state detonation or eventual extinction.

Charges which would sustain a steady detonation would be expected to have smaller velocity decay rates than charges which could not sustain a steady detonation.

To measure the decay rate from the oscilloscope trace, a computerized method of data reduction was devised in which the voltage-time profile was converted to a smooth velocity-distance curve suitable for analysis. Discrete points (about 25) along the oscilloscope trace were converted using a pencil follower to digitalized input data, punched onto paper tape. This information, along with appropriate time and resistance wire calibration constants for the conversion of voltage drop to distance along the charge, were treated by a finite difference method to yield discrete velocity-distance data. This was accomplished by defining the velocity, D_i, at the ith point as

$$D_i = \frac{x_{i+1} - x_{i-1}}{t_{i+1} - t_{i-1}}, \tag{7}$$

where x_i and t_i are the distance and time of the ith point, respectively.

The resulting set of D_i and x_i data was then curve-fit by an empirical expression,

$$D(x) = D_o \exp(-Bx).^{11} \tag{8}$$

Here, D_o can be interpreted as the initial velocity of the overdriven wave, and B the detonation-velocity decay constant (for example, cm^{-1}). The whole procedure of data reduction, including graphing equation 8, was carried out with a program developed for the Bureau's CDC 1700 computer.

Figures 3 and 4 illustrate some typical curves obtained by this procedure. It is readily seen that the decay constant B for the pulverized AN-FO mixture is less than that for the corresponding prilled AN-FO mixture. For comparison purposes, figure 5 depicts the detonation velocity of a catalyzed AN-FO charge which essentially achieved steady detonation, and figure 6 depicts the shock velocity-distance curve obtained from a PETN booster acting on an inert charge of sand (that is, without detonation). Some 30 velocity-distance profiles were determined in this way, and the relative probable error of the curve fit was less than 20 pct.

As indicated above, the constant B reflects, in a relative manner, the stability of the detonation wave, which itself is influenced by factors such as geometry, size, loading density, confinement, etc. Hence, B is a useful parameter for correlating the influence of these factors on toxic fume production.

---

[11] "exp" refers to exponential to naperian e.

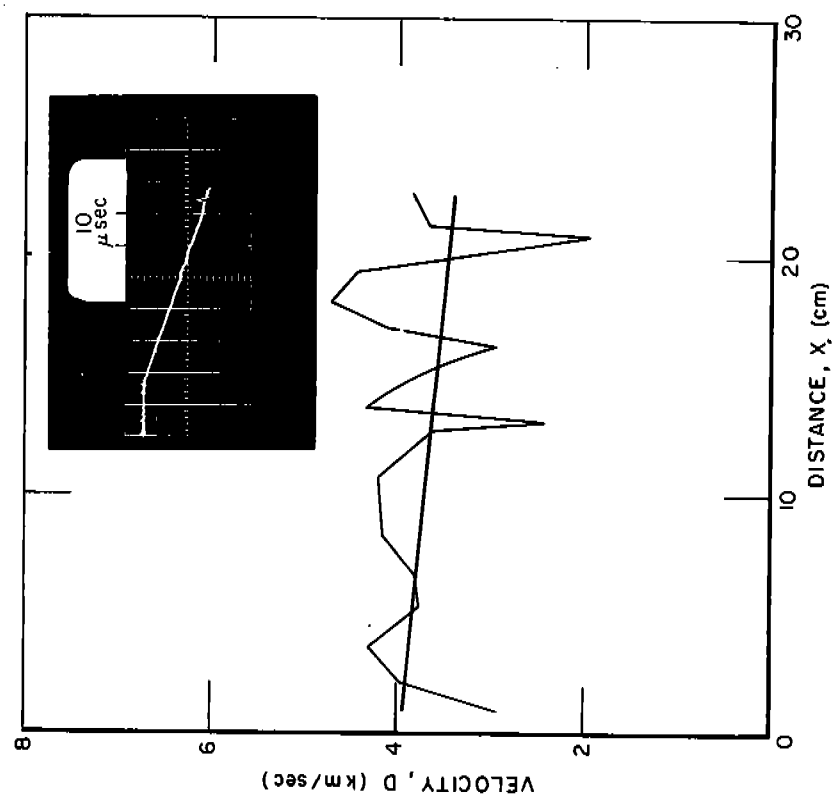

FIGURE 4. - Decay of detonation velocity AN-FO (pulverized) (94 to 6); D(X) = 3.95 exp [-0.00681 X], km/sec.

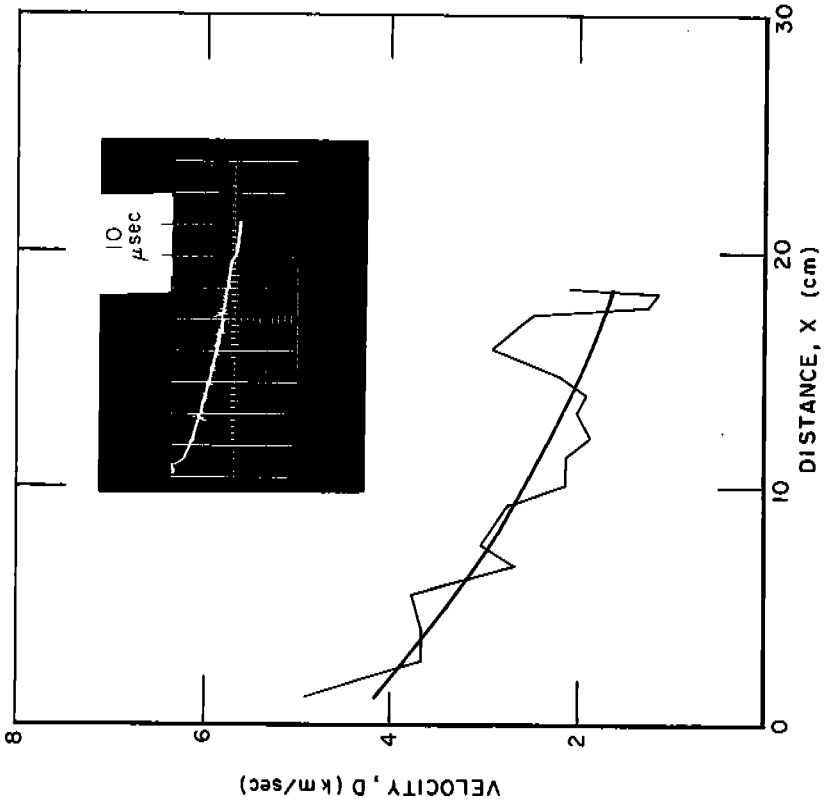

FIGURE 3. - Decay of detonation velocity AN-FO (prilled) (94 to 6); D(X) = 4.09 exp [-0.0504 X], km/sec.

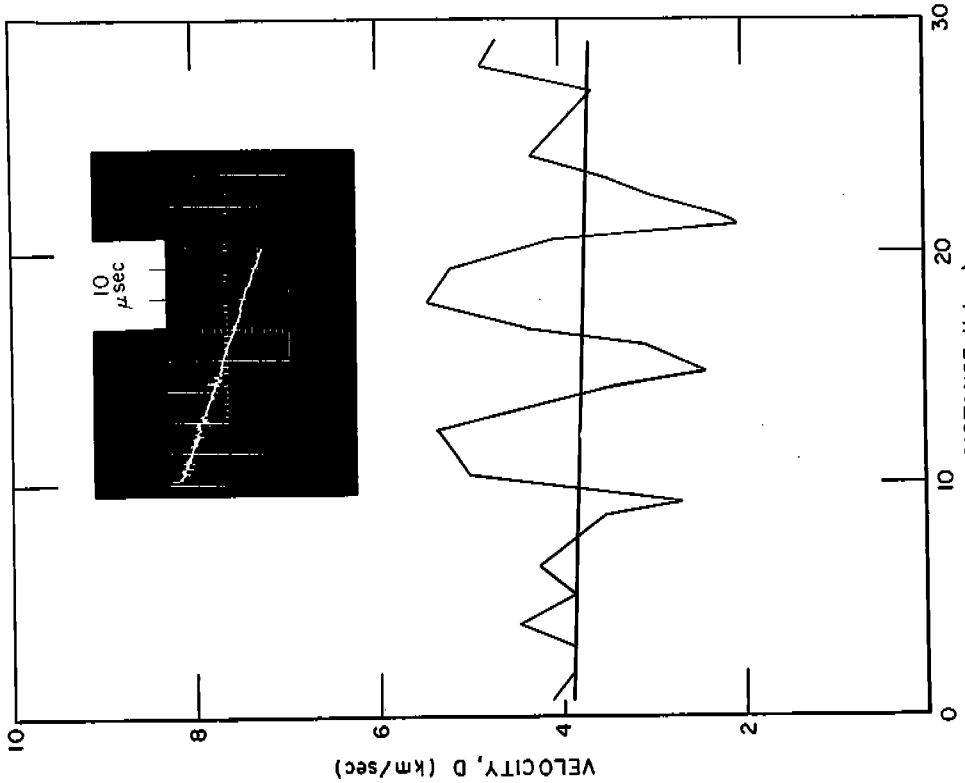

FIGURE 5. - Decay of detonation velocity catalyzed AN-FO (96 to 4) (equivalent); D(X) = 3.90 exp [-0.00238 X], km/sec.

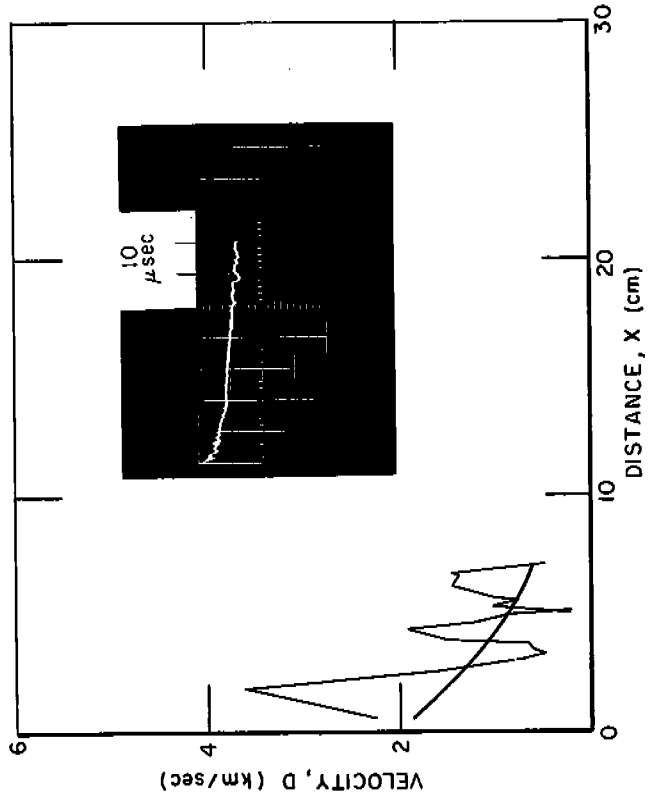

FIGURE 6. - Decay of shock velocity sand (inert charge); D(X) = 2.04 exp [-0.171 X], km/sec.

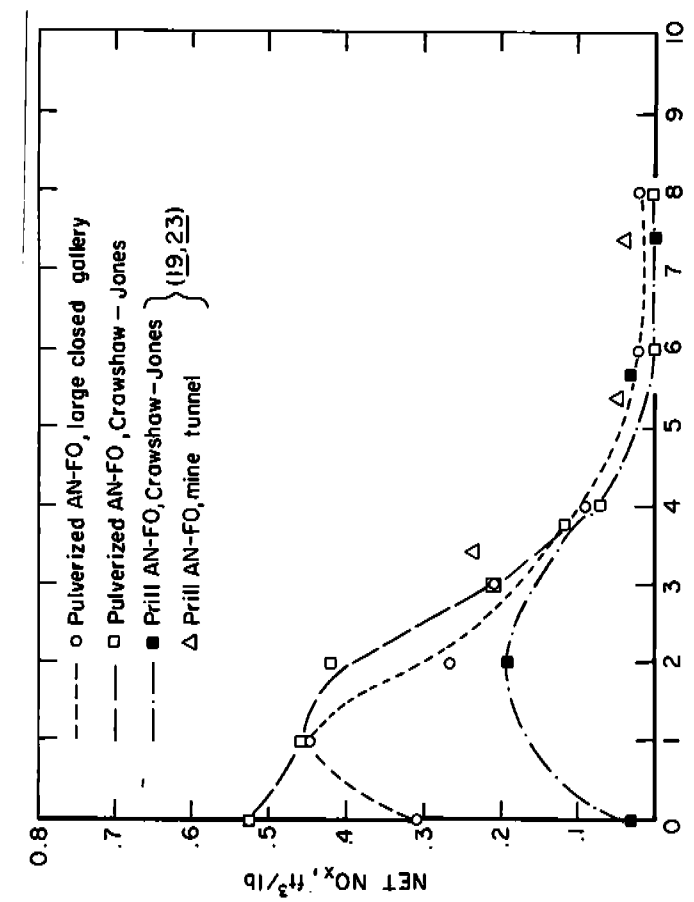

FIGURE 7. - Toxic fumes from AN-FO mixtures, gallery and theoretical results.

FIGURE 8. - Toxic fumes from AN-FO mixtures, gallery and Crawshaw-Jones results.

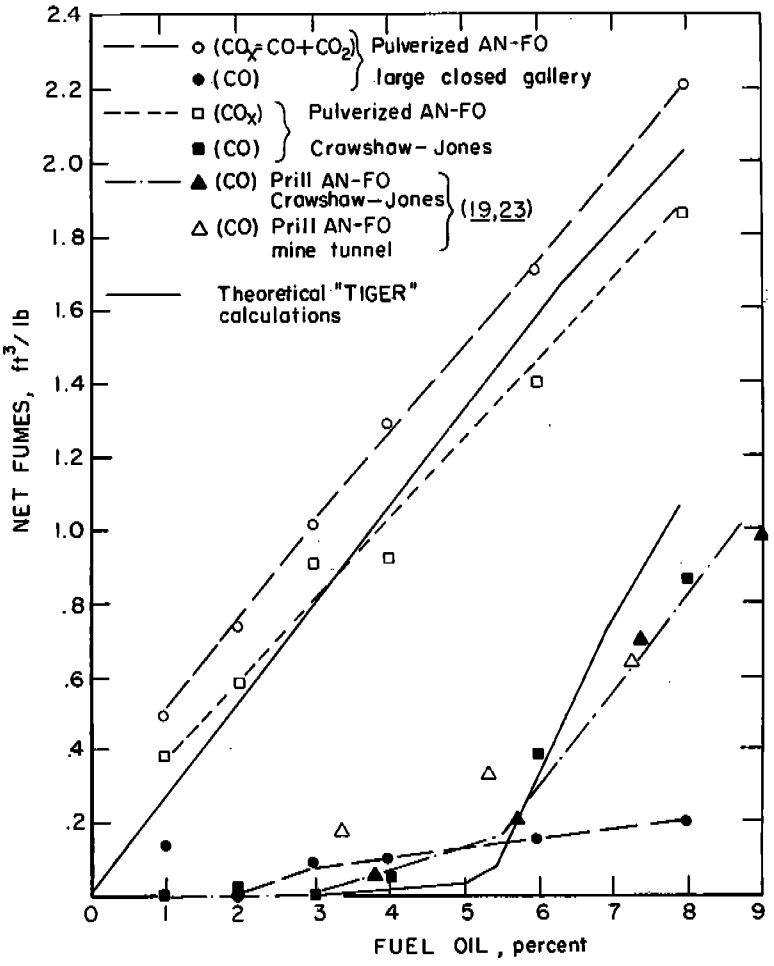

FIGURE 9. - Toxic fumes from AN-FO mixtures, carbon monoxide.

RESULTS AND DISCUSSION

A compilation of the results of the large closed-gallery and Crawshaw-Jones tests is shown in tables 3 and 4. The net toxic-fume production includes corrections to account for the presence of CO, NO, NO_2, and CO_2 fumes which arise from extraneous sources, for example, from the PETN booster, carbonaceous construction materials such as tape, and normal air in the gallery prior to firing. These corrections were accomplished in the following manner:

1. The CO and CO_2 observed from the zero percent AN-FO charges (that is, those containing no fuel oil) were considered to arise from all extraneous sources. The average concentrations of these species were then subtracted from values obtained from charges which contained oil.

2. The NO_x toxic fume production from PETN was determined in separate experiments (tables 3 and 4), and its value, normalized to the booster weight, was subtracted from the AN-FO results. In general, this latter correction is small.

Figures 7 and 8 illustrate the variation of net NO_x concentration as a function of fuel oil content. Several different curves are depicted. Figure 7 shows a theoretical curve based upon the "TIGER" calculations given in table 2, and two experimental curves representing the averaged results of the current large gallery tests for both pulverized and prilled AN-FO; figure 8 compares data from the large gallery test with current and previous (19) Crawshaw-Jones data. In addition, three data points are shown which refer to a previous mine tunnel test (23). Figure 9 depicts the available CO and CO_x (= CO + CO_2) fume data in a similar manner.

TABLE 3. - Large closed-gallery results for prill and pulverized AN-FO mixtures

Shot number	Percent fuel oil	ρ_o, g/cm^3	Net ft^3/lb						B, m^{-1}	D_o, km/sec	[1]D (14), km/sec
			NO	NO_2	NO_x	CO, std	CO_2	CO_x			
PRILL AN-FO--BLANK: NO = 0.003; NO_2 = 0.002; NO_x = 0.005; CO = 0.29; CO_2 = 2.13; CO_x = 2.42 STD FT^3											
10	0	0.76	0.06	0.07	0.13	0	0	0	16.9	5.1	0.7
16	1	.77	.12	.28	.39	-.03	.53	.51	5.9	3.2	1.4
11	2	.77	.11	.28	.38	-.06	.74	.69	4.6	3.3	1.7
23	3	.79	.12	.20	.31	-.16	.88	.73	5.1	3.7	1.8
21	4	.80	.10	.08	.18	-.11	.81	.70	5.5	4.2	2.0
12	6	.81	.05	.02	.07	-.02	1.06	1.04	5.0	4.1	2.1
13	8	.83	.02	.005	.03	.25	1.80	2.05	1.0	2.8	2.4
PULVERIZED AN-FO--BLANK: NO = 0.003; NO_2 = 0.002; NO_x = 0.005; CO = 0.09; CO_2 = 1.85; CO_x = 1.95 STD FT^3											
14	0	0.73	0.09	0.24	0.33	-0.01	0.09	0.08	9.9	4.6	1.2
15	0	.73	.09	.21	.30	.01	-.09	-.08	12.2	5.3	.9
19	1	.77	.14	.27	.41	.08	.41	.49	5.0	4.6	2.3
22	1	.74	.13	.36	.49	.18	1.15	(1.33)	3.7	4.1	2.4
25	2	.75	.12	.14	.26	.04	.64	.69	2.2	4.3	3.2
32	2	.81	.10	.13	.23	-.01	.83	.83	3.2	4.5	2.9
33	2	.82	.10	.13	.22	-.01	.53	.53	1.1	4.0	3.4
45	2	.83	.10	.16	.26	.04	.58	.62	.87	3.5	3.1
54	2	.82	.09	.12	.21	-.03	1.04	1.01	2.2	4.0	2.9
30	3	.74	.11	.10	.21	.08	.92	1.01	1.3	4.1	3.4
17	4	.74	.06	.02	.08	.09	1.00	1.09	2.0	5.1	3.8
18	4	.74	.09	.02	.11	.11	1.36	1.47	1.6	4.1	3.3
26	6	.75	.02	.01	.03	.14	1.71	1.82	1.7	4.6	3.6
27	6	.75	.01	.004	.02	.14	1.44	1.58	1.2	4.2	3.6
28	8	.76	.01	.01	.02	.20	1.92	2.12	1.9	4.8	3.7
29	8	.76	.01	.003	.02	.20	2.09	2.29	2.4	5.0	3.6
39	PETN[2]	1.4	.01	.01	.02	.05	8.56	8.60	-	-	-
40	PETN[2]	1.4	.03	.01	.05	.05	7.74	7.78	-	-	-
44	PETN[2]	1.4	.02	.02	.04	.10	7.62	7.72	-	-	-
50	PETN[2]	1.4	.02	.04	.06	.09	6.96	7.06	-	-	-
31	Sand	1.77	-	-	-	-	-	-	17.1	2.0	.6

[1]Velocity at 14 cm from booster-charge interface except for shots No. 10 (12 cm) and No. 31 (7 cm).

[2]Fume data are uncorrected for extraneous nitric oxides and carbon.

TABLE 4. - Crawshaw-Jones test results for pulverized AN-FO mixtures

Shot number	Percent fuel oil	ρ_o, g/cm^3	Net std ft^3/lb		CO_2	CO_x
			NO_x[1]	CO		
PULVERIZED AN-FO--BLANK: $NO_x = 3\times10^{-5}$; CO = 0.047: CO_2 = 0.996 STD FT^3						
8	0	0.71	0.59	0.02	0.006	0.03
10	0	.72	.48	-.005	-.01	-.02
12	0	.72	.52	-.01	.02	.01
15	1	.91	.47	-.008	.44	.43
21	1	.91	.45	-.03	.34	.31
9	2	.74	.43	.03	.51	.54
11	2	.73	.39	.004	.55	.55
13	2	.73	.43	.03	.63	.66
16	3	.92	.19	.02	.95	.97
22	3	.94	.23	-.01	.87	.86
17	4	.93	.05	.06	.91	.97
23	4	.94	.09	.02	.83	.85
18	6	.89	.0006	.53	1.03	1.56
24	6	.93	.0001	.25	.96	1.21
19	8	1.00	.0003	.86	.99	1.85
14	PETN	1.40	.0002	1.75	4.52	6.27
20	PETN	1.40	.0003	1.51	4.82	6.33
25	PETN	1.40	.0006	2.68	3.96	6.64

[1] NO_x determined by colorimetric method; B. A. Coulehan and H. Lang, Rapid Determination of Nitrogen Oxides With Use of Phenoldisulfonic Acid. Environ. Sci. and Technol., v. 5, 1971, pp. 163-164.

When comparing the current measured and theoretical NO_x curves, it is seen that only semiquantitative agreement exists between them. The predicted maximum value of NO_x fume production is in reasonable agreement with experiment; however, the peak in the experimental curve occurs at 1 to 2 pct FO whereas the predicted peak is at 3 to 4 pct FO. This result suggests that the virial EOS may not be totally adequate for describing the detonating state of AN-FO. Alternatively, the discrepancy could be related to the effects of increased nonideal detonation at the smaller fuel oil compositions. This point will be discussed further later in this section.

The fact that the shape of the theoretical curve follows the general shape of the experimental curves, and that the numerical values are of the same order of magnitude, lends some support to our assumption that the NO_x is frozen near its detonation-state concentration. It should be pointed out that this conclusion does not necessarily imply that NO and NO_2 each remain at their detonation state value. It is possible that the reaction

$$2NO + O_2 \text{ (air)} \rightarrow 2NO_2$$

can occur to some extent during and after expansion of the borehole gases into

the gallery air. This occurrence would explain in part the fact that the observed NO/NO_2 ratios are consistently smaller than the predicted ratios (table 5). However, for hazards evaluation purposes it is the total NO_x concentration which is significant, and this value would be independent of the extent of the above air oxidation reaction.

TABLE 5. - Comparison of predicted and experimental NO/NO_2 ratios for pulverized AN-FO

Percent FO	Theoretical NO/NO_2	Experimental NO/NO_2
0	5.9	0.42
1	10.0	.44
2	15.2	.77
3	23.6	1.1
4	38.9	3.2
5	82.6	-
6	1060	2.4
7	5500	-
8	10^4	2.5
9	2×10^4	-
10	2×10^6	-

The occurrence of a similar reaction between CO and gallery air during expansion, for example,

$$2CO + O_2 \text{ (air)} \rightarrow 2CO_2,$$

can also affect the observed CO fume production. Strong evidence that this occurs in the gallery can be seen from figure 9. Here we note that the CO_x net fume data are in reasonable agreement with theory. In fact, if the CO_x blank for pulverized AN-FO (that is, the gross CO_x measured for the zero percent FO charge) is increased by 10 pct, the experimental net CO_x data would almost coincide with the theoretical curve, suggesting a good experimental total carbon balance. On the other hand, the gallery test data for CO with fuel-rich compositions ($\geq$6 pct FO) fall well below the theoretical curve and the Crawshaw-Jones curve. In the latter test, the products expand into vacuum ($\sim$10 torr), and little air oxidation of CO should occur. Indeed the observed CO values for this test do agree reasonably well with theory. All these results point strongly to the occurrence of postdetonation oxidation of CO in the gallery test.

Unlike the case of NO_x, it is of considerable importance from a hazards viewpoint whether carbon appears as CO or CO_2 in the expanded detonation products. Thus it would appear that the atmospheric air expansion chamber used in the gallery may not be totally suitable for evaluating CO fume production. It is interesting to note in figure 9 that the three mine tests appear to fall more in line with the Crawshaw-Jones results than with the gallery results, in spite of the fact that the mine test involves product expansion into air. At this time, no good explanation exists for this

occurrence; however, postoxidation would not be expected to be reproducible except under carefully controlled test conditions.

Returning to figure 8, we see that the current gallery and Crawshaw-Jones tests with pulverized AN-FO yield very similar results for NO_x except for the zero percent fuel oil composition. As will be described later, the discrepancy at zero percent fuel oil is probably due to inadequate propagation of detonation rather than to the different test procedures. The apparent similarity of results of the two test methods was rather surprising since it was anticipated that condensed water, which always appears in the cooled products from the Crawshaw-Jones test, would absorb NO_x gas and hence give rise to a misleading low yield of NO_x. This potential problem might be indicated if one simply compares the current prill AN-FO gallery data with the previous prill AN-FO Crawshaw-Jones data. (See fig. 8.) However, these two sets of data refer to different explosive charge configurations (prepackaged charge and tamped borehole charge) which likewise might account for the observed results.

Some evidence for a lower value of NO_x yield in the Crawshaw-Jones test can be seen with the pulverized AN-FO containing 6 and 8 pct fuel oil. (See tables 3 and 4.) The Crawshaw-Jones data for NO_x yield are 10^{-3} to 10^{-4} ft^3/lb, whereas the NO_x data from the gallery are about a factor of 100 higher.

It is to be noted however that these particular data are derived from the measurement of rather small concentrations of NO_x; about 1 ppm in the gallery and about 100 ppm in the Crawshaw-Jones apparatus. The analytical measurements in each case (NO_2^* chemiluminescence for the gallery test and colorimetric for the Crawshaw-Jones test) are near their lower limits of reliability. Hence, the observed increase in NO_x yield in the gallery with the 6 and 8 pct compositions may be due to the different analytical procedures rather than to the different expansion chambers. In any case, such small yields of NO_x fumes are generally not considered hazardous for mining applications.

Contrary to our results with CO, the three NO_x mine test data points tend to follow the gallery curve and the Crawshaw-Jones curve. (See figs. 7 and 8.) The significance of this agreement is somewhat questionable, but it does support the hypothesis that laboratory tests for NO_x fumes can be extrapolated to mine conditions.

It is interesting to compare the amount of NO_x fumes produced by the prill AN-FO with that produced by the pulverized AN-FO (fig. 7). Although the two fume profiles are quite similar, there appears to be a significant increase in NO_x with the prill AN-FO at oil concentrations greater than 1 pct. Examination of the velocity decay rates and measured velocities for the two types of AN-FO (figs. 10-11) reveals that, in the current charge configuration, the prill AN-FO is less able to sustain a steady detonation than the pulverized AN-FO.

In fact, the values of the detonation velocity decay constant, B, and the detonation velocity at 14 cm, D (14), for the prill AN-FO (100/0), when compared to that of an inert sand charge, indicates a complete absence of detonation reaction; for the pulverized AN-FO (100/0), only partial reaction in the

overdriven wave is indicated. Since significant NO_x was found for these relatively nondetonating systems, it suggests that the AN must have partially decomposed during or after ejection from the cannon borehole. This, then, could also explain the large difference in the NO_x yield from the gallery and Crawshaw-Jones tests of the zero percent FO composition. Postdetonation reactions during or after expansion into air and vacuum would not be expected to be the same. On the other hand, the two types of AN-FO at 1 pct FO exhibit almost the same decay rate constants and the same NO_x fume production. These results are in concurrence with what has long been known in practice, namely, that inadequate initiation and propagation of detonation of AN-FO charges will result in higher NO_x fume production (14).

The apparent relationship between increased NO_x fumes with increased rarefaction losses (provided detonation does occur) suggests the possible alternative explanation for the observed difference between the theoretical and experimental curves of figure 7. If rarefaction losses increase with decreasing fuel concentration, as suggested by the observed decay rates and the values of the detonation velocity approximately midway through the charge (figs. 10-11), then the increase in NO_x because of this factor may be sufficient to shift the peak in the composition profile to lower fuel oil concentrations (for example, 1 to 2 pct). Unfortunately, this hypothesis cannot be evaluated much further experimentally since there are limitations on the size of charges that can be fired in the available laboratory tests.

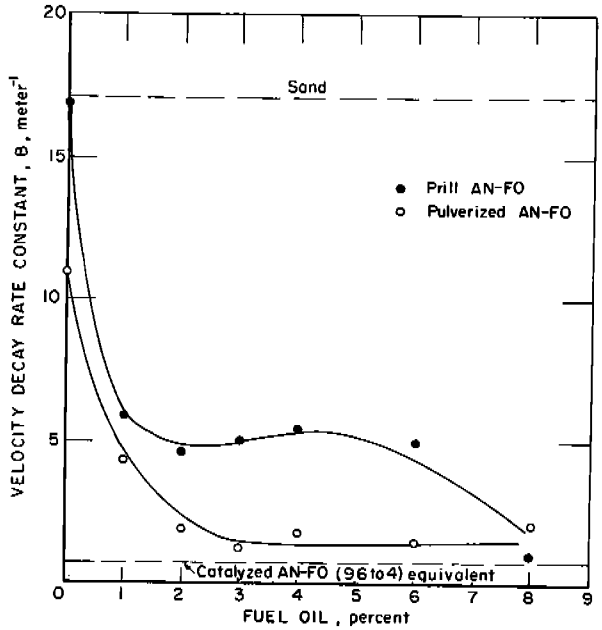

FIGURE 10. - Variation of velocity decay constant with variation in percent fuel oil.

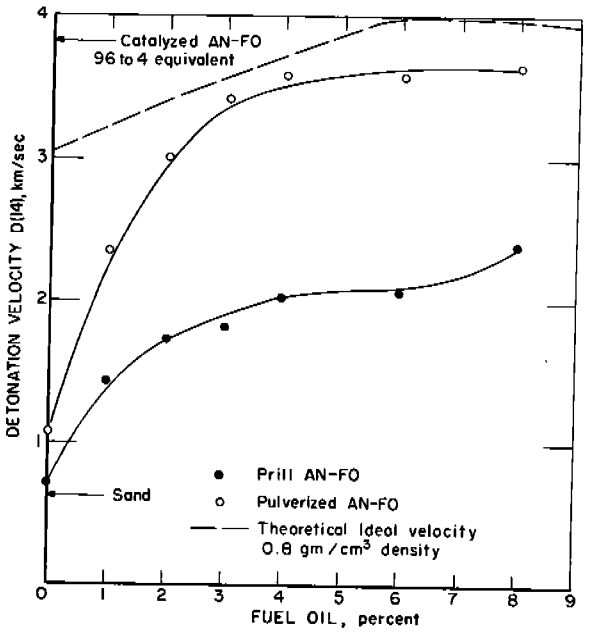

FIGURE 11. - Variation of detonation velocity at 14 cm with variation in percent of fuel oil.

CONCLUSIONS AND RECOMMENDATIONS

Several factors are clearly seen in the results of the current study. First, the Crawshaw-Jones and large closed-gallery tests lead to similar estimates of the NO_x fumes produced by an explosive in the test condition and probably in the mine condition. However, the use of the large closed-gallery test apparently brings to light a problem in determining CO fumes, namely that of obtaining meaningful data on CO yield. The oxidation of CO as the detonation products expand into the air has an appreciable effect on the observed values and interpretation of the data. Although air oxidation of CO also occurs under mine conditions, its extent would not be expected to be very reproducible. Under these circumstances, it would seem that the best that can be offered by any toxic fume test would be an accurate determination of the maximum amount of CO formed without air oxidation. An accurate determination could be accomplished in the large closed-gallery test if the air in the expansion chamber were replaced by vacuum (as in the Crawshaw-Jones test) or by nitrogen. Unfortunately, such replacement would be difficult because of the excessive pumping and/or purging requirements. However, a chamber approximately seven times smaller than the current one could still allow expansions sufficient to minimize water condensation and possible wall loss of NO_x. Such a chamber ($\sim 10^4$ l or ~ 350 ft^3) would require only 10 l of liquid N_2 per shot for purging purposes.

Second, the possibility of predicting toxic fume production in simple explosives has been demonstrated. Although the "TIGER" calculations with the virial EOS were not in exact agreement with experimental values, they did indicate the trends observed with compositional variations, and they did yield values of NO_x which approximated the experimental results. Owing to post-detonation oxidation of CO during product expansion into air, the calculated CO values could not be compared with the large gallery experimental values; however, reasonable agreement was obtained between the calculated and Crawshaw-Jones values for CO. This agreement suggests the possibility that, even with the current EOS, it may be possible to predict the maximum CO to be obtained from a given explosive composition.

Third, the amount of toxic fumes from AN-FO depends upon the nonideal detonation behavior of the explosive charge system. The velocity-decay rate constant was found to be a useful experimental parameter for correlating toxic fume production with the degree of nonideal detonation. This measurement should be employed in toxic fume tests whenever the detonation properties of explosives are sensitive to confinement and size conditions. It might also be pointed out that from the viewpoint of increased explosive yield and lower toxic fumes, pulverized AN-FO would be preferable to prilled AN-FO for use in small diameter blasting.

REFERENCES

1. Andreyev, K. K, and A. F. Belyayer. Theory of Explosive Substances. Moscow (1960). English translation FTD-MT-64-242, 1966, p. 574; available from National Technical Information Services, Springfield, Va., AD 643597.

2. Cook, M. A. Ch. in The Science of High Explosives. Reinhold Publishing Corp., New York, 1958, pp. 61-90.

3. Cowan, R. O., and W. T. Ficket. Calculation of the Detonation Properties of Solid Explosives With the Kistiakowsky-Wilson Equation of State. J. Chem. Phys., v. 24, 1956, p. 932.

4. Dow Chemical Company, Thermal Research Laboratory. JANAF Thermodynamic Tables. 1970, unpaged.

5. Fontijn, A., A. J. Sabadell, and R. J. Ronco. Homogeneous Chemiluminescent Measurement of Nitric Oxide With Ozone. Anal. Chem., v. 42, 1970, pp. 575-579.

6. Gordon, S., and B. J. McBride. Computer Program for Calculation of Complex Chemical Equilibria Compositions, Rocket Performance, Incident and Reflected Shocks, and Chapman-Jouquet Detonations. NASA SP-273, 1971, 245 pp.

7. Harzt, D., A. Kirsch, H. Seidel, and E. Ulrich. Experimental Determination of the Volume and the Toxic Components of Fumes in a 10 m^3 Chamber. 14th Internat. Conf. Mine-Safety Research Establishments, Donetsk, U.S.S.R. (1971); Safety Mine Res. Establishment (England) Translation No. 6024.

8. Hirschfelder, J. O., C. F. Curtiss, and R. B. Bird. Ch. in Molecular Theory of Gases and Liquids. John Wiley & Sons, Inc., New York, 1954, pp. 131-273.

9. Levine, H. B., and R. E. Sharples. Operator's Manual for Ruby. University of California, Lawrence Radiation Laboratory UCRL-6815, 1962, 123 pp.

10. Mason, C. M., and E. G. Aiken. Methods for Evaluating Explosives and Hazardous Materials. BuMines IC 8541, 1971, 48 pp.

11. Newhall, H. K. Kinetics of Engine-Generated Nitrogen Oxides and Carbon Monoxide. 12th Internat. Symp. on Combustion, The Combustion Institute, Pittsburgh, Pa., 1969, pp. 603-613.

12. Quinot, E., and C. Claeys. Nitrous Fumes From the Gases of Mining Explosives (Abstract). Proc. 14th Internat. Cong. Occupational Health, Madrid, v. 4, No. 288, 1963, pp. 961-964 (English translation).

13. Ribovich, J., R. W. Watson, and F. C. Gibson. Instrumented Card-Gap Test. AIAA J., v. 6, 1968, pp. 1260-1263.

14. Rossi, B. D. Control of Noxious Gases in Blasting Work, and New Methods of Testing Industrial Explosives. Vzryvnoe Delo Collection No. 68/25, Izdatel'stvo "Nedra" Moscow (1970), U.S. Department of Interior Translation TT 70-50163; available from National Technical Information Services, Springfield, Va., I PST, Catalog No. 5836.

15. Sax, N. I. Dangerous Properties of Industrial Materials. Reinhold Book Corp., New York, 3d ed., 1968, pp. 822, 962, and 968.

16. Streng, A. G. Evaluation of Toxic After-Detonation Gases Formed by Industrial Explosives. Explosivstoffe, No. 34, 1971, pp. 58-64.

17. Taylor, J. Detonation in Condensed Explosives. Oxford University Press, 1952, 196 pp.

18. Tiffany, E., J. Murphy, and N. E. Hanna. Comparison of Poisonous Gases From Permissible Explosives as Obtained in Bichel-Gage and Coal-Mine Tests. BuMines RI 4663, 1950, 12 pp.

19. Tournay, W. E., E. J. Murphy, G. H. Damon, and R. W. Van Dolah. Some Studies in Ammonium Nitrate-Fuel Oil Compositions. Univ. Mo. School Mines and Met. Bull., Tech. Ser. No. 97, 1959, pp. 164-174.

20. Van Dolah, R. W., F. C. Gibson, and J. N. Murphy. Further Studies on Sympathetic Detonation. BuMines RI 6903, 1966, 35 pp.

21. _____. Sympathetic Detonation of Ammonium Nitrate and Ammonium Nitrate-Fuel Oil. BuMines RI 6746, 1966, 34 pp.

22. Van Dolah, R. W., N. E. Hanna, E. J. Murphy, and G. H. Damon. Further Studies on Ammonium Nitrate-Fuel Oil Compositions. Univ. Mo. School Mines and Met. Bull., Tech. Ser. No. 91, 1956, pp. 90-101.

23. Van Dolah, R. W., E. J. Murphy, and N. E. Hanna. Fumes From Ammonium Nitrate-Hydrocarbon Mixtures, ed. by G. B. Clark. Internat. Symp. on Min. Res., v. 1, Pergamon Press, New York, 1961, pp. 77-89.

24. Wiebenson, W. E., Jr., W. H. Zwisler, L. B. Seely, and S. R. Brinkley, Jr. TIGER Computer Program Documentation. Stanford Res. Inst. Rept. on Contract DA-04-200-AMC-3226(x), 1968, 394 pp.

* U.S. GPO: 1974—705-457/598

INT.-BU.OF MINES,PGH.,PA. 19112